AIAA-95-1608-CP

PERFORMANCE MODEL FOR REVERSIBLE FLUID BALLOONS

by Jiunn-Jenq Wu and Jack A. Jones
Jet Propulsion Laboratory
California Institute of Technology
Pasadena, California 91109

Abstract

The ALtItude Control Experiment (ALICE) is a balloon system that consists of a helium lifting balloon and a buoyancy-controlling freon R114 balloon. Condensation of freon gas in the cooler upper atmosphere and vaporization of liquid freon in the warmer lower atmosphere can be effectively used to adjust the net buoyant force so that the balloon system may float between desirable ranges of altitudes.

This report summarizes efforts to produce an analytical model to predict the performance of this type of altitude control balloon in the earth's atmosphere. Various interactive parameters that are influential to the dynamics of the system were identified and treated. The analytical model developed herein correlated well with three ALICE day flight trajectories and one ALICE night flight trajectory in the earth's atmosphere. A similar approach can be applied to the design of a Venusian balloon system that could repeatedly travel to the lower, hot altitudes or surface of Venus for imaging or science experiments and then float higher in order to cool the electronics.

I. Introduction

The concept of using the phase change of a fluid to control a balloon altitude in the atmosphere of Venus was originally conceived by Moskalenko et al.[1] in 1978 and was expanded by JPL in 1993 [2] to apply to the atmospheres of other planets, including earth. In summary, a phase change fluid may be used in a planetary atmosphere to produce a net change of buoyancy. In the warmer lower atmosphere, the fluid evaporates and fills a balloon, thereby displacing more air and creating a net gain in buoyancy, allowing the balloon to rise. In the cooler upper atmosphere, the fluid condenses, thereby creating a net decrease in buoyancy that allows the balloon system to descend.[3] Understanding the operational characteristics of such a balloon system on Earth is essential for designing one to be used in the Venusian atmosphere.

A comprehensive test program known as the ALtItude Control Experiment (ALICE) was initiated in July of 1993 to prove the basic principles.[4] After careful considerations of industrial safety and environmental concerns, freon R114 was selected as the controlling fluid. However, since freon gas is heavier than air, the addition of a helium balloon was necessary to provide the necessary lifting force.

The decision to use R114 as the controlling fluid posed a technical challenge. Since R114 gas is very heavy (molecular weight = 170.9), it cannot displace a large volume of air, and therefore cannot produce a large lifting force for a given weight. Therefore, for a balloon system to float at a neutrally buoyant altitude with 1 kg of partially liquefied R114, the helium balloon must provide a lift in the narrow range of 0.83 to 1 kg. This margin must be maintained regardless of the dry weight of the system. Therefore, this margin will be a smaller percentage compared to the helium lift as the dry weight of the system increases.

The control margin, expressed in terms of the ratio of the control force due to phase change of R114 to the net lift of the helium gas, is generally on the order of 10% or less for the ALICE flights. Since the control margins are small, a variety of factors can easily upset the delicate force balance of the balloon system and prevent a successful flight. These factors include the effect of thermal radiative and convective heat transfer on balloon fluid temperatures, leakage of the balloon fluids, and the rates of freon condensation and evaporation. For example, the first two balloons launched by JPL at UCLA in July of 1993 demonstrated reduced lift near the condensation altitude but failed to descend. An analysis of the flight trajectory of ALICE 0/B indicated that a full condensation of R114 probably occurred, but solar heating of the helium gas might have produced a lift that exceeded the range of forces controllable by the freon balloon.

Since the condensation and vaporization of R114 cannot produce a dominant control force, other related parameters that can alter the dynamics of the balloon system must be investigated. Analytical studies on a helium balloon were performed by Carlson and Horn [5]. This work provided an excellent starting point for the present investigation.

II. Outline Of The Theory

Equation of Motion

The equation of motion closely follows that of Carlson and Horn [5]. The balloon system consists of a primary (helium) lifting balloon and a buoyancy-controlling secondary (freon) balloon as illustrated in Figure 1. Generally, the secondary balloon contains superheated freon gas and subcooled freon liquid. Therefore, a three-balloon analytical model is required to describe the motion of the altitude control balloon system. The three-balloon model consists of a primary (helium) balloon, a gaseous freon balloon, and a liquid freon balloon. Its motion is governed by the following relation:

$$(m_{sys} + c_m \rho_a V)\frac{d^2 z}{dt^2} = g(\rho_a V - m_{sys}) - \frac{1}{2}\rho_a c_D \left(\frac{dz}{dt} + W_z\right)\left|\frac{dz}{dt} + W_z\right| A_p \qquad (1)$$

where,

$$m_{sys} = m_{tot} - \int_o^t (\dot{\pounds}_p + \dot{\pounds}_s)\, dt \qquad (2)$$

$\dot{\pounds}_p$ = helium leak rate (primary balloon)

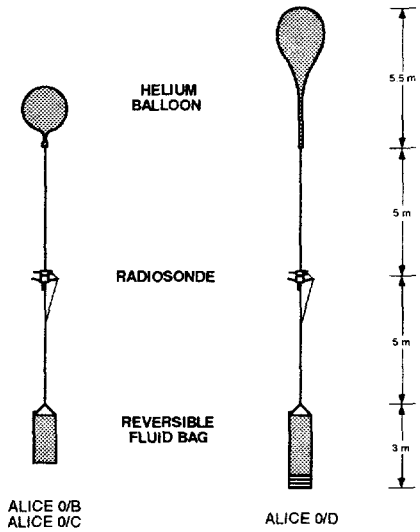

Figure 1. Atitude control experiment balloon system.

$\dot{\pounds}_s$ = freon leak rate (secondary balloon)

$$V = V_p + V_{sg} + V_{sl} \tag{3}$$

Heat Balance

$$\frac{dQ_{pg}}{dt} = \dot{q}_{pg} - \rho_a V_p g \frac{dz}{dt} - \dot{\pounds}_p c_{p,\mathrm{He}} T_{gp} \tag{4}$$

$$\frac{dQ_{pf}}{dt} = \dot{q}_{pf} \tag{5}$$

$$\frac{dQ_{sg}}{dt} = \dot{q}_{sg} - \rho_a V_{sg} g \frac{dz}{dt} - \dot{\pounds}_s \frac{Q_{sg}}{m_s} \tag{6}$$

$$\frac{dQ_{sl}}{dt} = \dot{q}_{sl} - \dot{\pounds}_s \frac{Q_{sl}}{m_s} \tag{7}$$

$$\frac{dQ_{sf}}{dt} = \dot{q}_{sf} \tag{8}$$

Heat Flux

The primary balloon shape is nearly spherical for ALICE 0/B and ALICE 0/C. The heat flux equations can be written as:

$$\dot{q}_{pf} = [G\alpha_{pweff}\left(\frac{1}{4} + \frac{1}{2}r_e\right) + \varepsilon_{pint}\sigma(T_{gp}^4 - T_{fp}^4) + CH_{pgf}(T_{gp} - T_{fp}) + CH_{pfa}(T_a - T_{fp}) - \varepsilon_{pweff}\sigma T_{fp}^4 + \varepsilon_{pweff}\sigma T_{BB}^4]S_p \tag{9}$$

and

$$\dot{q}_{pg} = [G\alpha_{pgeff}(1 + r_e) + \varepsilon_{pint}\sigma(T_{gp}^4 - T_{fp}^4) - CH_{pgf}(T_{gp} - T_{fp}) - \varepsilon_{pgeff}\sigma T_{gp}^4 + \varepsilon_{pgeff}\sigma T_{BB}^4]S_p \tag{10}$$

Since the balloon film is semitransparent, the effective thermal radiative properties due to "greenhouse" effects can be described as [5]:

$$\alpha_{pweff} = \alpha_{pw}\left(1 + \frac{\tau_{pwsol}(1 - \alpha_{pg})}{1 - r_{pwsol}(1 - \alpha_{pg})}\right) \tag{11}$$

$$\varepsilon_{pint} = \frac{\varepsilon_{pg}\,\varepsilon_{pw}}{1 - r_{pw}(1 - \varepsilon_{pg})} \tag{12}$$

$$\varepsilon_{pweff} = \varepsilon_{pw}\left(1 + \frac{\tau_{pw}(1 - \varepsilon_{pg})}{1 - r_{pw}(1 - \varepsilon_{pg})}\right) \tag{13}$$

$$\alpha_{pgeff} = \frac{\alpha_{pg}\,\tau_{pwsol}}{1 - r_{pwsol}(1 - \alpha_{pg})} \tag{14}$$

$$\varepsilon_{pgeff} = \frac{\varepsilon_{pg}\,\tau_{pw}}{1 - r_{pw}(1 - \varepsilon_{pg})} \tag{15}$$

As shown in Figure 1, the secondary balloon is basically a rectangular polyethylene bag before it is filled with freon. Therefore, when the balloon is inflated, the shape may not be spherical. In order to avoid overestimating the radiative heat transfer, however, and to obtain a solution independent of the balloon orientation, a spherical thermal radiation heat transfer model similar to that of the primary balloon is used to analyze the secondary balloon. This is a reasonable simplification since thermal radiative properties of a gas depend on the thickness of the gas layer and the thermal radiative heat transfer rate depends on the shape factor between the radiation source and the receiving body. The thermal radiative heat transfer surface area for the secondary balloon then becomes:

$$S_s = \pi D_s^2 \tag{16}$$

where

$$D_s = \left(\frac{6}{\pi} V_s\right)^{1/3} \tag{17}$$

Enhanced convective heat transfer is desirable to accelerate condensation and vaporization of the freon gas to achieve a rapid altitude control. Therefore, a different aerodynamic shape of the secondary balloon must be used to reflect the realistic design. If the aerodynamic surface area of the gaseous part of the secondary balloon is S_{sg}, then the heat flux equations are:

$$\dot{q}_{sf} = [G\alpha_{sweff}\left(\frac{1}{4} + \frac{1}{2}r_e\right) + \varepsilon_{sint}\sigma(T_{gs}^4 - T_{fs}^4) - \varepsilon_{sweff}\sigma T_{fs}^4 + \varepsilon_{sweff}\sigma T_{BB}^4]S_s + [CH_{sgf}(T_{gs} - T_{fs}) + CH_{sfa}(T_a - T_{fs})]S_{sg} \tag{18}$$

and

$$\dot{q}_{sg} = [G\alpha_{sgeff}(1 + r_e) + \varepsilon_{sint}\sigma(T_{gs}^4 - T_{fs}^4) - \varepsilon_{sgeff}\sigma T_{gs}^4 + \varepsilon_{sgeff}\sigma T_{BB}^4]S_s - CH_{sgf}(T_{gs} - T_{fs})S_{sg} \tag{19}$$

As with the primary balloon, the effective thermal radiative properties of the secondary gaseous balloon can be expressed similar to eqns. (11-15).

For the secondary balloon shown in Figure 1 (ALICE 0/C), the polyethylene bag has a length L and a width W before filling. The aerodynamic surface area is approximately:

$$S_{sg} \approx 2\,L\,W \tag{20}$$

Upon condensation, the liquid freon is assumed to stay at the bottom of the polyethylene bag and form a half horizontal cylinder. In this case, the half cylinder has a diameter:

$$D_{sl} = \left(\frac{8}{\pi}\frac{V_{sl}}{W}\right)^{1/2} \tag{21}$$

and a surface area:

$$S_{sl} = \frac{\pi}{2} W D_{sl} \tag{22}$$

Since this area is small, thermal radiative heat transfer is probably small compared to convective heat transfer, and this area is thus used to analyze both modes of heat transfer. Also, since the heat capacity of the liquid is considerably larger than that of the polyethylene film containing it, the heat content of the secondary liquid balloon can be approximated by that of the liquid freon only. The temperature of this liquid balloon is then equal to the temperature of the liquid freon. This assumption is adequate in view of the low heat flux for the "slow" moving balloon and the adequacy of nucleate boiling characteristic of the liquid freon. The only contribution of the polyethylene film is to reduce the effective absorptance and emittance of the freon liquid. Therefore, the heat flux equation for the liquid part of the secondary balloon (ALICE 0/C) is:

$$\dot{q}_{sl} = [G\alpha_{sleff}\left(\frac{1}{2} + r_e\right) + \varepsilon_{sleff}\sigma(T_{BB}{}^4 - T_{ls}{}^4) + CH_{lfa}(T_a - T_{ls})]S_{sl} \tag{23}$$

Convective Heat Transfer Coefficients

1. Primary balloon film-to-air — sphere [5]

Nusselt number for forced convection:

$$Nu_1 = 0.37\, Re^{0.6} \quad (V_p < 53800) \tag{24a}$$

$$Nu_1 = 0.74\, Re^{0.6} \quad (V_p \geq 53800) \tag{24b}$$

Nusselt number for free convection:

$$Nu_2 = 2 + 0.6(Gr\, Pr_a)^{1/4} \tag{25}$$

Nusselt number for primary balloon film-to-air convection:

$$Nu = \text{Max}\{Nu_1, Nu_2\} \tag{26}$$

2. Primary balloon helium-to-film — sphere [5]

Nusselt number:

$$Nu = 2.5(2 + 0.6\, Rn^{1/4}) \quad Rn < 1.34681 \times 10^8 \tag{27a}$$

$$Nu = 0.325\, Rn^{1/3} \quad Rn \geq 1.34681 \times 10^8 \tag{27b}$$

3. Secondary gas balloon film-to-air — vertical flat plate [6-8]

Reynolds number: $Re = \dfrac{\rho_a L\,|U_z + \text{Wz}\,|}{\mu_a}$ (28)

Nusselt number for forced convection in air ($Pr_a = 0.71$):

$$Nu_1 = 0.5924\, Re^{1/2} \quad Re < 487508.3 \tag{29a}$$

$$Nu_1 = 0.033\, Re^{0.8} - 758.3 \quad Re \geq 487508.3 \tag{29b}$$

The Nusselt number for free convection can be evaluated as follows [6]:

$$Nu^T = 0.515\, Rn^{1/4} \tag{30a}$$

$$Nu_l = \frac{2.8}{ln\left(1 + \dfrac{2.8}{Nu^T}\right)} \tag{30b}$$

$$Nu_t = 0.103\, Rn^{1/3} \tag{30c}$$

$$Nu_2 = \left[(Nu_t)^6 + (Nu_l)^6\right]^{1/6} \quad 1 < Rn < 10^{12} \tag{30d}$$

Nusselt number for secondary balloon film-to-air convection:

$$Nu = \text{Max}\{Nu_1, Nu_2\} \tag{31}$$

4. Secondary balloon R114 gas-to-film — vertical flat plate [6]

The Nusselt number can be calculated as follows:

$$Nu^T = 0.515\, Rn^{1/4} \tag{32a}$$

$$Nu_l = \frac{2.8}{ln\left(1 + \dfrac{2.8}{Nu^T}\right)} \tag{32b}$$

$$Nu_t = 0.103\, Rn^{1/3} \tag{32c}$$

$$Nu = \left[(Nu_t)^6 + (Nu_l)^6\right]^{1/6} \quad 1 < Rn < 10^{12} \tag{32d}$$

5. Secondary liquid balloon film-to-air —horizontal cylinder [8]

Nusselt number for forced convection in air ($Pr_a = 0.71$):

$$Nu_1 = 0.38 + 0.44\, Re^{1/2} \quad Re < 1297.742 \tag{33a}$$

$$Nu_1 = 0.22\, Re^{0.6} \quad Re \geq 1297.742 \tag{33b}$$

Nusselt number for free convection in air ($Pr_a = 0.71$):

$$Nu_2 = \left[0.6 + 0.322(Rn)^{1/6}\right]^2 \tag{34}$$

Nusselt number for secondary balloon film-to-air convection:

$$Nu = \text{Max}\{Nu_1, Nu_2\} \tag{35}$$

Atmospheric Model

The current altitude control balloon is designed to operate inside the troposphere of the Earth's atmosphere, where the ambient temperature decreases linearly with increasing altitude until the tropopause (about 11 km). Between the troposphere and the mesosphere (altitude > 40 km) is the stratosphere, which is characterized as having a constant temperature of approximately - 55°C. Using these two characteristics of the atmosphere and the perfect gas law, the temperature and pressure distributions inside the troposphere and the stratosphere can be described by the following relations [9,10]:

Troposphere (altitude $z < z_{tropopause}$):

$$T_a = T_{sea\ level} + \frac{dT_a}{dz} z \tag{36}$$

$$P_a = (A - B\,z)^n \tag{37}$$

Stratosphere (altitude $z \geq z_{tropopause}$):

$$T_a = T_{tropopause} \approx -55°C \tag{38}$$

$$P_a = P_{a,tropopause} \exp(a - b\,z) \tag{39}$$

Since aviation weather data are available in a tabulated form, these atmospheric constants can easily be obtained in conjunction with the specified set of weather data.

The atmospheric model can be modified to include the inversion layer found in the Los Angeles basin. This can be done by assuming that the temperature is uniform within the inversion layer. In this situation, the temperature slope of the troposphere must be evaluated using the temperature data at an altitude above that of the inversion layer and below that of the tropopause.

The blackball model of Reference 5 representing the Earth-air infrared radiative input to the balloon system was adopted for the present analysis. Normally, T_{BB} decreases linearly from a ground (inside inversion layer) value about 5.5 K below the ambient temperature to a value at the tropopause. Above the tropopause, T_{BB} is assumed to be constant. The blackball temperature above the tropopause for low altitudes and/or thick clouds is:

$$T_{BB} = 214.4 - 0.20 \cdot (\% \text{ of cloud cover}) \tag{40}$$

For thin, high cirrus clouds:

$$T_{BB} = 204.4K$$

And the Earth's reflectivity (albedo) is:

$$r_e = 0.18 + 0.0039 \cdot (\% \text{ of cloud cover}) \tag{41}$$

Gas, Liquid, and Balloon Film Thermal Radiative Properties

The thermal radiative properties of polyethylene and helium gas are listed in Reference 5. Additional thermal radiative properties that are essential to the present analysis were measured at JPL using spectral data, and appear in Table 1.

Generally, the spectral data was measured for wavelengths between 300 nm and 2500 nm, which is sufficient to evaluate the solar radiative properties of a material. For infrared radiative properties, additional spectral data measurements were made to extend the wavelength to 18.3 μm.

Table 1. Radiative Surface Properties

	Solar		Infrared	
Material	Absorptance	Reflectance	Emittance	Reflectance
Polyethylene	.001	.114	.031	.127
Latex Rubber[1]	.0445	.251	.15[2]	.10[2]
Helium Gas	.003	—	.0003	—
R114 Gas	.00184	—	.60	—
R114 Liquid	.003[2]	—	.95[2]	—

1. 175% linear stretched
2. Estimated

Other Parameters

The virtual mass coefficient C_m is assumed to be 0.5[3]. A drag coefficient $C_D = 0.8$ correlated well with flight data. A standard solar constant, $G = 1396$ W/m^2 = 2 cal/cm^2 min, is also used.

Phase Separation of the Secondary Balloon

The secondary balloon consists of a liquid balloon and a gaseous balloon in the same bag. The temperature of the gas is generally different from that of the liquid. After receiving heat or undergoing an altitude change, some liquid may evaporate to produce gas whose temperature may be different from that of the pre-existing gas. Similarly, after rejecting heat or changing altitude, some gas may condense to produce liquid whose temperature may be different from that of the original liquid pool. This newly produced liquid will mix with the original liquid to form a new liquid pool, or newly formed gas will mix with the original gas to form a new gaseous balloon state.

II. Solution Approach

Equations (1), (14) - (18), and

$$\frac{dx}{dt} = -\,w \sin\theta \tag{42}$$

$$\frac{dy}{dt} = -\,w \cos\theta \tag{43}$$

$$\frac{dz}{dt} = U_z \tag{44}$$

complete a system of nine first-order differential equations describing the motion of the balloon system, where w is the prevailing wind speed and θ is the wind direction (measured clockwise from north).

Numerical solutions of this set of equations can be performed to obtain the three-dimensional balloon coordinates in terms of flight time. The numerical method used in the present investigation is either simple stepwise linear integration, or Runge-Kutta 4th-order methodology. Since most of the present calculations require a 2-second numerical integration step to assure the desired numerical stability, and the Runge-Kutta 4th-order method can not improve the accuracy of the results with this fine step, using the simple linear integration method is sufficient to obtain an accurate and reliable solution.

The most frequently encountered numerical instability in performing this integration is an overestimation of the interchange heat transfer rate between the balloon gas and the balloon film. The exchange of heat between the balloon gas and the balloon film is accomplished by thermal radiation and free convection heat transfer, as described earlier. This heat exchange rate can easily be overestimated and results in an unreasonable oscillation of balloon film and gas temperatures. This instability can be partially alleviated by imposing a constraint derived from the first law of thermodynamics, by limiting the maximum interchange heat exchange rate to a value that will establish a thermal equilibrium between the gas and the film at the conclusion of the heat exchange process. Although this method is effective to some extent, it may not eliminate the problem completely. In that event, a smaller integration step size is required to continue the numerical

integration and to yield a reasonable solution. Further investigation is necessary to improve this numerical scheme.

The computer code was written in Microsoft Excel, Version 4.0, which is usable by both Windows and Macintosh platforms. Two input worksheets are used to describe the basic balloon parameters and the atmospheric model. A macro sheet is used to perform the numerical integration. Data generated by the macro sheet computation is recorded in an output worksheet. Since various charts are linked to the output worksheet, the results of the numerical calculation can be displayed either in a tabulated or graphical form.

III. Discussion

The driving force of the balloon system is the net lifting term of Eq. (1), $g\,(\rho_a V - m_{sys})$. Since the volume displaced by the liquid freon is small, its contribution to the lifting force is negligible. The lifting force thus takes the form:

$$\text{Lift} = g\left\{ m_p\left[\left(\frac{R_p}{R_a}\right)\left(\frac{T_{gp}}{T_a}\right) - 1\right] + m_s\left(\frac{R_s}{R_a}\right)\left(\frac{T_{gs}}{T_a}\right)\left(\frac{m_{gs}}{m_s}\right) - \left(m_s + m_{dry}\right)\right\} \quad (45)$$

The first term of the equation is the net lifting force provided by the helium gas. The second term is the buoyant force for the freon gas, which is the altitude control force. The third term is the dead weight, which consists of the dry weight of the balloon system and the total weight of the freon (gas and liquid).

If the balloon is traveling upward in the troposphere, the freon gas will reject heat to the lower ambient temperature and condense. Condensation reduces the mass fraction of the freon gas, and thus reduces the lift of the system. On the other hand, if the balloon is traveling downward, the freon liquid will absorb heat and evaporate. Evaporation of liquid freon increases the mass fraction of freon gas, and thus increases the lift of the system. Therefore, condensation and evaporation of freon provide the necessary restoring force for the balloon system to stay at a floating altitude. This altitude control scheme can be effective only when the restoration force is large enough to reverse the direction of the system lift, however. In other words, if the balloon system is traveling upward, the net system lift must be negative before full condensation of freon gas occurs. Similarly, if the balloon is traveling downward, the net system lift must be positive before full vaporization of freon liquid occurs.

Under an idealized condition that $T_{gp} = T_{gs} = T_a$, Equation 45 for a helium/R114 balloon system can be reduced to:

$$Lift/g = 6.238\, m_p + 0.1695\, m_s\left(\frac{msg}{ms}\right) - (m_s + m_{dry}) \quad (46)$$

Therefore, the buoyant control force is only 1.66N (Lift/g = 0.170 kg) per kilogram of freon. Since the control force is small, the helium leak must be strictly controlled to sustain a prolonged flight. Also, the effect of thermal radiative heat transfer on the temperature of the helium gas must be carefully evaluated, so that proper helium fills can be selected to assure a successful flight.

IV. Test Results

ALICE 0/B

ALICE 0/B was a day flight altitude control balloon system launched at 10 a.m. on July 29, 1993 from UCLA. The breakdown of the system mass is indicated in Table 2. The post-flight analysis suggests that the freon gas was fully condensed at an altitude of about 10,150 m before reaching the tropopause at about 12,345 m. The balloon system continued to travel upward into the stratosphere, where the ambient temperature was about -55°C. Three hours after launch, the balloon climbed to an altitude of 13 km and terminated data transmission. Due to a lack of flight data, the trajectory after 3 hours of flight was unknown. However, the present theory indicates that the balloon continued to travel upward. Due to the decrease in pressure in a uniform temperature stratosphere, the freon liquid would start to vaporize at an altitude of about 22.4 km and accelerate the ascent of the balloon system (Figure 2). Although the balloon had a free lift of only 1.19N (Lift/g = 121 g) when measured in the shade just before launch, as

Table 2. ALICE 0/B, C, D Weight Breakdowns

ALICE 0/B	Gas (grams)	Film (grams)	Payload (grams)	Total (grams)
Primary Balloon (Helium)	249.43	303.4	1.8	554.63
Secondary Balloon (Freon R114)	996	109	9.4	1114.4
Radiosonde Assembly			184.1	184.1
TOTAL				1853.13

ALICE 0/C	Gas (grams)	Film (grams)	Payload (grams)	Total (grams)
Primary Balloon (Helium)	333.92	303.4	162.7	800.02
Secondary Balloon (Freon R114)	1001.2	115.5	84.5	1201.2
Radiosonde Assembly			396.5	396.5
TOTAL				2397.72

ALICE 0/D	Gas (grams)	Film (grams)	Payload (grams)	Total (grams)
Primary Balloon (Helium)	409	815	104	1328
Secondary Balloon (Freon R114)	1000	157	48.5	1205.5
Radiosonde Assembly			471.9	471.9
TOTAL				3005.4

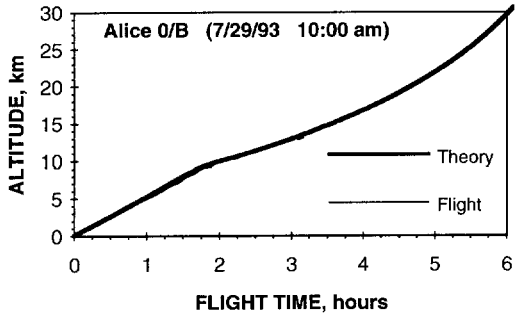

Figure 2. ALICE 0/B altitude vs time

calculated from Eq. (46), it is very likely that the effect of solar heating of the helium balloon was underestimated, so that ALICE 0/B was overfilled with helium. The excessively filled helium balloon produced a system lift beyond the control margin of the freon balloon.

ALICE 0/C

ALICE 0/C was designed to validate the concept of achieving altitude control of a balloon system by the condensation of freon gas, and to verify the accuracy of the newly formulated theory. The secondary balloon was a simple rectangular polyethylene. No efforts were made to accelerate the evaporation process of liquid freon. In order to eliminate the effect of solar heating, the balloon was launched at night (9:21 p.m.) on February 24, 1994 from JPL. Pre-launch calculations were made using an estimated dry weight of 1.006 kg and 1 kg of freon. The weather data were measured at Point Mugu at 4 a.m. on February 23, 1994. Thermal radiative properties of the balloon materials used in these calculations were either measured or estimated from the ALICE 0/B flight. Apparently, it is possible to select an appropriate helium fill to keep the balloon afloat overnight at an altitude below 14 km. The balloon would then ascend upon sunrise, due to solar heating.

A decision was made to launch the balloon system at a free lift (measured in a high bay near the launch site) of about 1.82 N (Lift/g = 185 g). Although this selected launching free lift appeared to exceed the maximum freon control force of 1.66 N, this level of helium fill was very conservative in view of analytical results for a night flight. The nature of this flight would be sufficient to demonstrate the condensation of freon gas as a means to control the balloon altitude, although the amount of helium carried on board and the heat transfer surfaces provided were insufficient to vaporize the liquid freon to regain the altitude during descent.

Using the actual flight system mass (Table 1), updated weather data, and slightly adjusted thermal radiative properties of balloon materials, the results of the post-flight analysis are shown in Figure 3. The correlations between the theory and the actual flight data are excellent. The ALICE 0/C flight achieved altitude control by the condensation of freon gas. The analytical model accurately predicted the behavior of the flight.

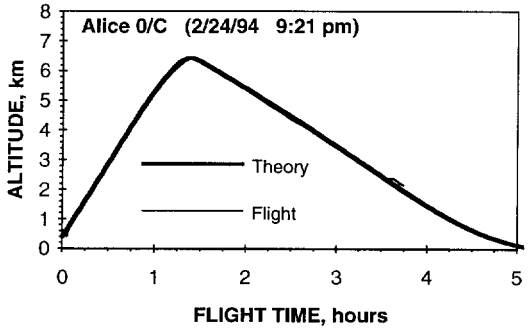

Figure 3. ALICE 0/C altitude vs time

ALICE 0/D

ALICE 0/D was launched at 9:03 p.m. on July 24, 1994, from JPL. The balloon system flew over the San Gabriel Mountains and the Mojave Desert, and was sighted at daybreak the next day at Daylight Pass on the northeast rim of Death Valley. Ground vehicle chase terminated at about 8:00 a.m. as the balloon flew over Nellis Air Force Range and the Nevada Nuclear Test Site. Data acquisition continued until loss of signal occurred at 11:20 a.m., July 25, as the balloon passed over the horizon. Actual flight data compared favorably with pre-launch model estimates of balloon behavior. Figure 4 shows data from actual flight in a thin line, and the post-flight analysis in a bold line. The topography under the ground track is constructed from the altitude data, wind profile, and terrain elevation obtained using Microcomputer Spectrum Analysis Model (MSAM) software and the terrain data base of the National Telecommunications and Information Administration (NTIA) and is shown at the bottom of Figure 4. Figure 5 compares the velocity derived from the flight altitude profile, using the method of least squares, and that of the post-flight analysis. Details of the balloon system design data can be found in Reference 4.

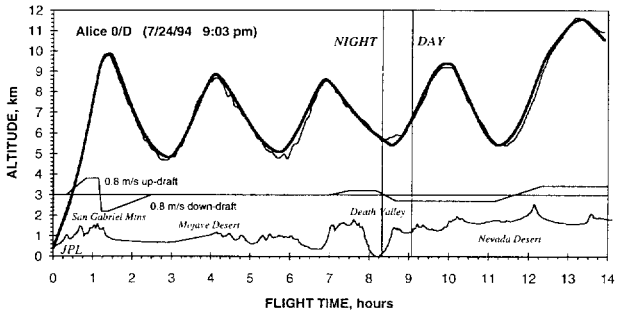

Figure 4. ALICE 0/D altitude vs time

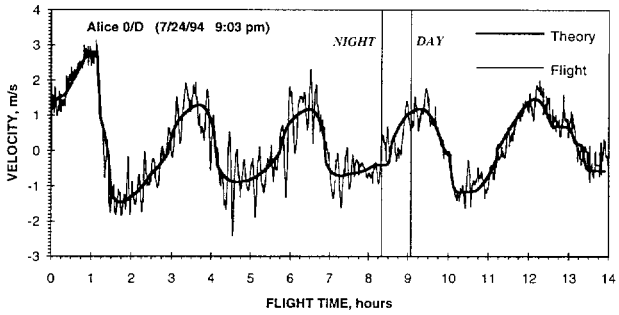

Figure 5. ALICE 0/D velocity vs time

The post-flight analysis indicates that

1. The performance of the pleated liquid freon heat exchanger can be accurately estimated by using a vertical flat-plate model and a porosity factor of the liquid (void to total volume) of about 30%. This is in line with the pre-launch estimate.

2. ALICE 0/D climbed to the first peak altitude about 30 minutes ahead of the prediction. The pre-launch calculation assumed a spherical helium balloon similar to the latex balloon used in the flight of ALICE 0/C. Since ALICE 0/D used a polyethylene bag for the primary helium balloon, the teardrop-shaped balloon significantly reduced the drag in the ascending phase of the motion. An ascending drag coefficient of 0.4 and a descending drag coefficient of 0.8

correlate well with the flight data. However, the reduction in drag alone can not fully explain the timing of the first peak. The correlation became successful when an updraft and a downdraft of 0.8 m/s on the windward side and leeward side of the San Gabriel Mountains were taken into account, as shown in the middle part of Figure 4.

3. The unusual behavior of the last recorded flight cycle shown in Figure 4 was due to the combined effects of a brief exposure of the balloon system to an intense reflected solar heating (albedo) and an updraft of about 0.43 m/s. In the middle of the first descending leg of the daylight flight, the albedo increased from a normal value of 0.18 to 0.278 for 90 minutes and then to 0.535 for 15-30 minutes. This change in albedo could be explained from the observed appearance of a low, white cloud over the horizon. The updraft was probably generated when the air stream flowed over the rough terrain and the thermal boundary layer created by the desert heating in the morning hours. The desert heating deserves special attention because the temperature in Death Valley was about 21°C at night and about 46°C at noon time.

4. ALICE 0/D acquired more than 14 hours of flight data. It is possible to correlate the actual leak rates of the balloon fluids to the pre-launch leak rate measurements. Generally, the leak rate depends on the surface area of the balloon, the pressure of the balloon fluid (equal to the partial pressure difference between the interior and exterior of the balloon surface). If the leak is due to permeation, the leak rate is proportional to a permeability constant, which is a function of temperature. The relationship between the proportional constant and the permeability constant was evaluated from the leak rate measured before launch. Permeation is not the only factor that controls the leakage of the balloon fluid. In order to separate its effects on the overall leak rate, a leak constant that is independent of temperature was also evaluated from the measured leak rate. The overall leak rate was calculated as the sum of the partial contributions of these two factors. The overall behavior of ALICE 0/D agrees well with the analytical model if 90% of helium leak in the primary balloon is attributable to permeation.

V. Summary and Conclusions

As a result of this effort, a thermodynamic model now exists for predicting the bobbing motion of phase-change balloons in the earth's atmosphere. A number of important things were learned during the course of this work. The first was that the balloon material's thermodynamic properties, especially solar absorptance, are very critical. Even the very small solar absorptance of 0.045 for latex rubber can make the difference between tropospheric bobbing or stratospheric popping for this type of phase-change balloon system. Second, fluid leak rates must be carefully measured for both the primary helium balloon and the phase-change freon balloon. Other important parameters in the model that were learned are the need to use a different coefficient of drag for ascent and descent, how changes in ground contour affect flight characteristics, and the necessity of accurately measuring gas temperatures in sunlight. The groundwork laid in the development of this unique model for phase-change balloons now makes it possible to make similar models for bobbing balloon systems for other gaseous atmosphere planets, as well as for Titan, a gaseous atmosphere moon of Saturn.

References

1. Moskalenko, G. M., "Mekhanika Poleta v Atmosfere Venery," Mashinasteroenie Publishers, Moscow, 1978.

2. Jones, Jack A., "Balloon Altitude and Temperature Control." JPL Notice of New Technology, NPO #19223, May, 1993.

3. Jones, Jack A. , "Reversible Fluid Balloon Altitude Control Concepts," AIAA Lighter Than Air Conference, Clearwater, Florida, Paper 95-1621, May 1995

4. Nock, Kerry, "Balloon Altitude Control Experiment (ALICE)," AIAA Lighter Than Air Conference, Clearwater, Florida, Paper 95-1632, May 1995

5. Carlson, L. A. and Horn, W. J., "New Trajectory Model for High-Altitude Balloons." J. Aircraft, Vol. 20, No. 6, June 1983.

6. Rohsenow, W. M., et al., *Handbook of Heat Transfer Fundamentals,* 2nd Ed. McGraw-Hill Book Co., 1985.

7. Rohsenow, W. M., et al., *Handbook of Heat Transfer Applications,* 2nd Ed. McGraw-Hill Book Co., 1985.

8. Holman, J. P., *Heat Transfer,* 4th Ed. McGraw-Hill Book Co. 1976.

9. Pope, A., *Wind Tunnel Testing,* 2nd Ed. John Wiley & Sons, Inc., 1954 (Appendix)

10. Dommasch, D. O., et al., *Airplane Aerodynamics.* Pitman Publishing Corp., 1957.

Nomenclature

A	cross-sectional area, m^2
c_f	specific heat of the balloon film, J/kg·K
c_P	specific heat at constant pressure, J/kg·K
C_D	coefficient of drag
CH	convective heat transfer coefficient, $W/m^2 \cdot K = Nu \times k/D$
C_m	virtual mass coefficient
D	characteristic length
g	acceleration due to gravity, m/s^2
G	solar constant, W/m^2
Gr	Grashof number= $g\beta\Delta TL^3/(\nu^2)$
h	enthalpy, J/kg
k	thermal conductivity. W/m·K
$\dot{m}$	leak rate, kg/s
L	length
m	mass, kg
Nu	Nusselt number
P	pressure, Pa
Pr	Prandtl number
$\dot{q}$	heat flux, W

r reflectance

R gas constant

Rn Rayleigh number = Gr x Pr

Re Reynolds number = $\rho DU/\mu$

S surface area, m^2

t time, s

T temperature, K

U velocity, m/s

V volume, m^3

W width

W_z downdraft, m/s

w wind speed, m/s

x,y,z balloon coordinates, m

α solar absorptance

ε infrared emittance

θ wind direction, deg

μ viscosity, Pa·s

ρ density, kg/m^3

σ Stefan-Boltzman constant = 56.69 $nW/m^2 \cdot K^4$

τ transmittance

ν kinematic viscosity = μ/ρ

Subscripts

a air or ambient

BB blackball

eff effective

f film

g gas

int interchange

l liquid

p primary balloon

s secondary balloon

sys balloon system

tot initial total

w balloon film or IR thermal radiative properties of balloon film

$w$sol solar thermal radiative properties of balloon film